Analysis and Simulation of Reliable and Robust UAV Data Transmission Through Geo Satellite using Long Code DSSS with ZP Algorithm

Ehsan Azizi [1], Mohammad Hossein Madani [2]
1- Electrical Engineering Faculty, Malek-Ashtar University of Technology, Lavizan, Tehran, Iran.
2- Electrical Engineering Faculty, Malek-Ashtar University of Technology, Lavizan, Tehran, Iran.
Email: madani@mut.ac.ir (Corresponding author)

ABSTRACT:
Wireless communication is the major form of connection nowadays. In most cases it exploits the benefits of the spread spectrum techniques to overcome corruptions introduced by channel like Doppler residual frequency, noise, interference and jamming. The purpose of this paper is to exchange secure information with unmanned aerial vehicle (UAV) through GEO satellites at low bit rates (kbps) with the aim of expanding the radius and operational coverage in the absence of LoS communications. In order to evaluate the possibility of communication, the link budget calculations are performed and minimum Carrier to Noise ratio (C/N) required to receive the signal at the receiver's side is measured. Basically, due to the information relay with geo-satellite, security of the link and the lack of access to information by unauthorized users is very important, therefore, direct sequence spread spectrum technique with long code has been used in physical layer to increase signal security and non-detectability. In order to detect the signal, different code acquisition techniques are examined and Zero Padding (ZP) is shown to outperform the other existing techniques in terms of Doppler effect tolerance and probability of detection in low SNRs. The results show that the proposed method makes detection at SNR levels as low as -14dB possible with a probability of false alarm of 10-5 and Pd>0.9.

KEYWORDS: SNR, Acquisition, UAV, Doppler, Zero Padding (ZP).

1. INTRODUCTION

Deployment of different means of wireless communication has become more widespread among different groups with different applications. From cell phones and wireless Internet to secure military communications. The propagation of radio waves in free spaces such as the urban environment, causes the waves to be reflected and reach the receiver from different paths. Additionally at each certain place and time, numerous users may request to make use of a specific frequency channel under a desired protocol. One way to deal with such problems is the use the spread spectrum technique. The basis of this technique is to spread the signal spectrum in the frequency domain beyond the actual need for the data contained in it. Satellite communications are the outcome of research in the area of communications and space technologies whose objective is to achieve ever-increasing ranges and capacities with the lowest possible costs. In this paper, the UAV is assumed to deploy the Spread Spectrum technique in order to increase the transmission of information over long distances, considering its extended range coverage, while using a public broadcasting satellite to relay links to UAV. Spread spectrum techniques are among the most commonly used techniques in communication systems today, since the use of these techniques will increase the securely of the signal layer.

Today, a lot of research has been done to robustly send data via UAVs and mobile receivers and many papers have been published in this field. [1] explores the paradigm that Remotely Piloted Air Systems (RPASs) or Unmanned Aerial Vehicles (UAVs) are integrated as a communication platform with cellular networks using radio access. [2] explores

Paper type: Research paper
https://10.71822/mjtd.2025.1092501
Received: 17 February 2024; Revised: 11 April 2024; Accepted: 20 June 2024; Published: 1 March 2025
How to cite this paper: E. Azizi, M. H. Madani, **"Analysis and Simulation of Reliable and Robust UAV Data Transmission Through Geo Satellite using Long Code DSSS with ZP Algorithm"**, *Majlesi Journal of Telecommunication Devices*, Vol. 14, No. 1, pp. 39-48, 2025.

tethered UAV assisted hybrid cooperative communication to improve the end-to-end performance of the links between base stations and user equipment. [3] examines potential data link candidates for unmanned aerial vehicles (UAVs). Authors in [4] put forward the UAV data link deployment scheme based on 5G technology after analyzing the shortcomings of traditional UAV data links, and analyse the key issues such as transmission rate, end-to-end delay and network coverage. [5] proposes an anti-interference scheme, named as Mary-MCM, for UAV data links in AGIVNs based on multi-array (M-array) spread spectrum and multi-carrier modulation (MCM). [6] characteristics of code division multiple access are used to realize the TT&C of the mass unmanned aerial vehicle. [10] the design and analysis of Telemetry, Tracking and Command Subsystem (TT&CS) for Libyan imaging mini-satellite (LibyaSat-1) is presented. The presented method in [7], called Segmented Zero Padding (SZP), reduces the Doppler effects on the probability of detection in the acquisition of GPS receiver. To improve the mean acquisition time performance of the zero-padding (ZP) method, [8] is proposed to fully exploit the computation capability of FFT by partially folding the local pseudo-noise (PN) code. In [9], an expression for the expected values of the cells' energies to analyze the impact of the Doppler bin width on detection and false alarm probabilities is presented. [10] presents a new onboard PN Codes Synchronizer Architecture based on the Generalized Zero Padding Algorithm (GZP) and frequency domain Doppler compensation. In [11], a fast acquisition algorithm is put forward for high dynamic DSSS signal based on double layers of short FFT. In [12], the widely used Zero Padding Scheme (ZPS) for direct GPS P-code acquisition is generalized to investigate the effects of the ZPS on detection performance, parallel searching capability, and mean acquisition time. [13] compares the meaning of different threshold setting principles in the code acquisition process of a direct sequence (DS) spread spectrum (SS) receiver. Finally, [14] indicates the standards of DVB-S and DVB-S2. What is analyzed in this paper is sending reliable and robust data through the geo satellite using the Zero Padding method to UAV, which has been done with the help of the introduced references. The structure of this paper includes problem definition in section 2, system model in section 3, and performance evaluation of the zero padding method in the section 4, and finally, section 5 contains the conclusion.

Fig. 1. Figure of network.

Table 1. Link Specifications.

Name	Value
Ku band Frequency	11-14 GHz
f_{uplink}	13.75 GHz
$f_{downlink}$	10.7 GHz
Satellite EIIRP	54.4 dB
Height of satellite	35814 Km
G/T Receiver	7 dB/k

2. PROBLEM DEFINITION

As previously mentioned in the introduction, spread spectrum techniques are used both to prevent the multipath fading phenomenon and also to increase the range of data transmission to the receiving stations while performing link budget calculations. This method requires significantly larger bandwidth than the original signal bandwidth because the signal processing gain is 30dB. Parameters related to DVB-S and SDVB-S2 standards have been performed for transplant budget calculations [14].

2.1. Calculation of the Minimum C/N

According to the DVB-S and DVB-S2 standard for link budget calculations, the BER value is less than 10^{-6} for BPSK and QPSK modulation schemes [14], and the minimum C/N ratio for signal detection needs to be calculated [19]. The minimum E_b/ N_0 value required for BER=10^{-6} is equal to 10.5dB. Since the received signal is BPSK modulated, the

occupied bandwidth of the signal using the RRC filter is 12KHz. In MPSK modulation scheme, to achieve a bit rate of 9.6 Kbps, a minimum of 19.2 KHz channel bandwidth is required [8]. This requirement can be further decreased. C/N ratio required to obtain the desired BER is obtained as follows:

$$50.32 = \left(\frac{C}{N}\right) + 10Log(2 \times 9600) \quad (3)$$

$$\left(\frac{C}{N}\right) = 7.5dB \quad (4)$$

2.2. Downlink Budget

In the current paper, the receiver, being a ship, car, UAV and etc. has been assumed to be mobile, which might possibly lead to Doppler effect. The downlink budget can be calculated to be $\frac{C}{N} = 34.3dB$ based on (3) [16].
The C/N obtained is greater than the calculated minimum C/N, so the downlink is established and the signal is detected in receiver.

2.3. Uplink Budget

The calculations in this section are similar to the calculations of the Downlink budget. BER for the uplink is considered to be 10^{-7} [14]. Firstly, as in the previous section, the minimum C/N required for the Uplink is calculated, which will be followed by the calculations for the uplink budget. The value of E_b/N_0 for BER=10^{-7} is equal to 11.5dB. The carrier to noise ratio can be calculated as:

$$\left(\frac{C}{N}\right) = 8.6 \quad (5)$$

minimum C/N value can therefore be obtained as follows [19][20]:

$$\frac{C}{N} = 42.78 \quad (6)$$

According to the obtained C/N, it can be concluded that the uplink has been established because it surpasses the minimum C/N.

2.4. Signal Model

The k-th sample of In-phase and Quadrature phase components of the received digital baseband signal are as follows:

$$s_I[k] = Ad[k+\tau]c[k+\tau]\cos(\omega_D k\Delta t + \varphi) + n_I[k] \quad (7)$$

$$s_Q[k] = Ad[k+\tau]c[k+\tau]\sin(\omega_D k\Delta t + \varphi) + n_Q[k] \quad (8)$$

Where A is the signal amplitude, d is the modulated data bit $\in \{-1, +1\}$, τ is the code phase offset of the received signal, c is the spreading code's chip $\in \{-1, +1\}$, ω_D is the residual frequency in radians, Δt is the sampling period (the same as code period i.e. one sample per chip), φ is the unknown carrier phase offset and n_I and n_Q are in-phase and quadrature phase additive white Gaussian noises respectively with zero mean and variance σ^2 , $\mathcal{N}(0, \sigma^2)$.
Codes used in spread spectrum system; It can be said that these codes cause the signal to become LPI. In other words, it makes access to information impossible for unauthorized individuals and receivers. This is achieved because, to gain access to the desired information, the exact same code used in the transmitter side must be used in the receiver side after full synchronization [15]. The basis of the spread spectrum technique is to expand the bandwidth of the transmitted signal. Considering the codes used in spread spectrum systems, which have a pseudo-noise property, it causes the signal to act similar to noise [15]. In this paper, 14th and 24th order code is used. In fact, security in physical layer proves the signal to be LPI and LPD, which is an intrinsic feature of all SS systems. To retrieve the signal in the receiver, it is necessary for the code to be completely synchronous with the received signal, since if the received signal is not synchronous with the code generator in the receiver due to transmission delay, detection would not be possible. So synchronization in the receiver will include two stages: acquisition and tracking. According to the codes used, there are many synchronization methods. For short codes there are series and parallel methods in the time domain that these methods cannot be used for codes with long periodicity, and so the acquisition methods in the frequency domain have

been used, which are the ZP, DF, XFAST method and Average method. In this paper, long codes have been used, so while reviewing the mentioned methods, select the ZP method and analyze and simulate the detection curves, acquisition time, system model of this method simulated by MATLAB Simulink. In Zero Padding method, it is assumed that the length of the FFT receiver L and the number of zeros added to the signal are represented by N [16],[17] so the steps of the Spread Spectrum method following:

1) The received signal is sampled at a rate equal to the chip rate and transmitted to the base band.
2) A piece with length L-N of the selected received signal, N zero is attached to it until its length reaches L, then its FFT conjugate is calculated.
3) A window with length L is viewed from the production code and its FFT is calculated.
4) IFFT The product of FFT is calculated two steps before and N + 1 of the first sample is considered as the result of correlation.
5) The maximum IFFT size result of the previous step is compared with the threshold, if it crosses the threshold, the acquisition is declared.[18]

In section3 system model is mentioned, which includes the transmitter, receiver, and finally, we will provide a review of the parameters related to the performance of the simulated method.

3. System Model

As a DS receiver starts to operate, the number of samples is removed from the received signal and the acquisition operation, Doppler search is performed on it, then in the tracking stage, go back to the received signal and samples its update is received and synchronized by the distributor code and deleted. At the beginning of the tracking stage, the time taken to acquire the code is considered and the code generator is moved forward as much as this time so as not to lag behind the received signal. Because during the acquisition phase, more recent samples of the received signal are not used and the offset amount obtained at the end of this phase is equal to the shift between the transmitted code and samples of the received signal, which was removed at the beginning of the receiver. The receiver in the current work, focuses solely on the acquisition of the signal.

3.1. Transmitter

Each bit of the transmitted signal, which has a rate of 9.6kbps is multiplied by 1024 chips, which is a sample of quasi-random code with rate 10MHz. Other specifications of the PRN code are given in Table1. The signal is then passed through the RRC filter in the transmitter and each symbol with 8 samples is ready to be sent to the AWGN channel. Fig. 2 shows the transmitted signal spectrum and Fig. 3 shows the channel model.

Table 2. Specifications of the PRN code [15]

Name	Value
Primitive Polynomial	$g(x) = x^{14} + x^{10} + x^6 + x + 1$
Binary Mode	[100010001000011]
Octal Mode	42103
Initial LFSR	[00000000000001]
Periodicity	$N = 2^{14}-1 = 16383$
Processing gain (G_P)	30dB

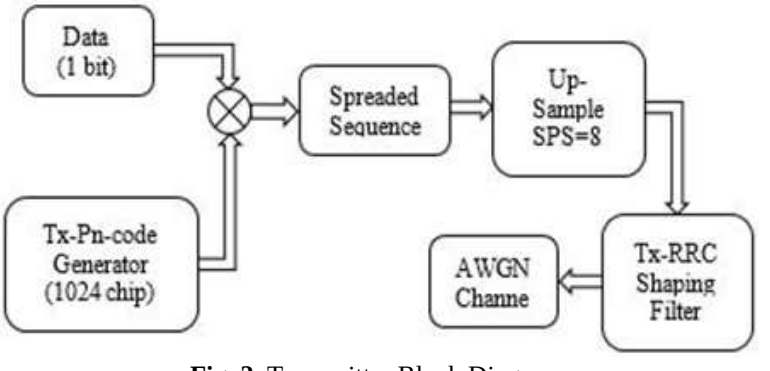

Fig. 2. Transmitter Block Diagram.

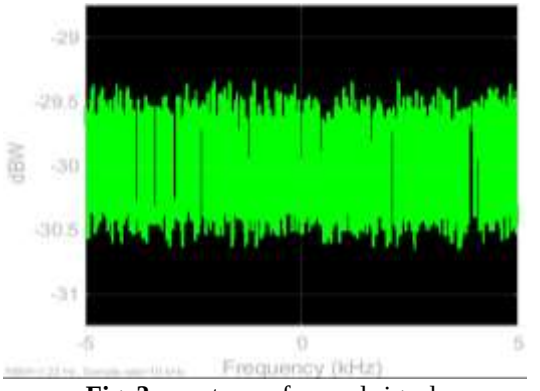

Fig. 3. spectrum of spread signal.

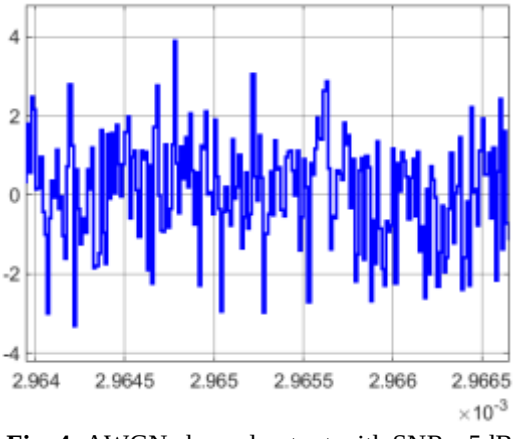

Fig. 4. AWGN channel output with SNR=-5dB.

3.2. Receiver

According to the block diagram of the receiver shown in Fig. 5, structure of the receiver is as follows:
RRC filter is placed at the beginning of the receiver to remove the transmitter shaping. The signal then enters the down sampling block to remove 8 samples per symbol. The method used to acquire the code in the receiver is ZP. In this method, the receiver picks up half of the FFT block, i.e., 512 samples, by the buffer from the received signal, and also picks up observation windows with a length of 1024 from the code generator in the receiver. The receiver pads 512 zeros to the 512 samples taken from the signal to reach a length of 1024, then takes FFT* and multiplies by 1024 samples of the output code from which the FFT is taken. This is followed by the IFFT of the signal in the previous stage (product of the received signal multiplied by the PRN code in the receiver's side). Subsequently, the maximum amount of IFFT is compared with the threshold. If the maximum value is higher than the threshold, the signal enters the tracking phase, otherwise the code generator is shifted by 1024 samples. This comparison is repeated until the maximum amount of IFFT surpasses the threshold.

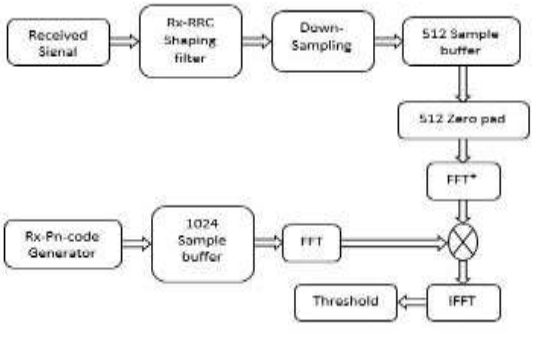

Fig. 5. Receiver Block Diagram.

3.2.1Threshold

The operation of the Tang detector method shown in Fig.4 is such that it takes an RMS value from the IFFT output, and multiplies the output by a value which depends on the SNR value in order for the threshold to surpass the signal level. The value of scale is obtained according to the noise level in this simulation. This scale is obtained in such a way that at SNR = -14dB, the P_d=0.9 [13].

Fig. 4 shows the threshold values and the maximum IFFT value. In each period of code (T_C), the maximum signal value is twice as much as the threshold value, which is exactly when the receiver code generator overlaps with the received signal. If in two consecutive correlations, the maximum signal value exceeds the threshold, it means that the Zero Padding method has worked correctly.

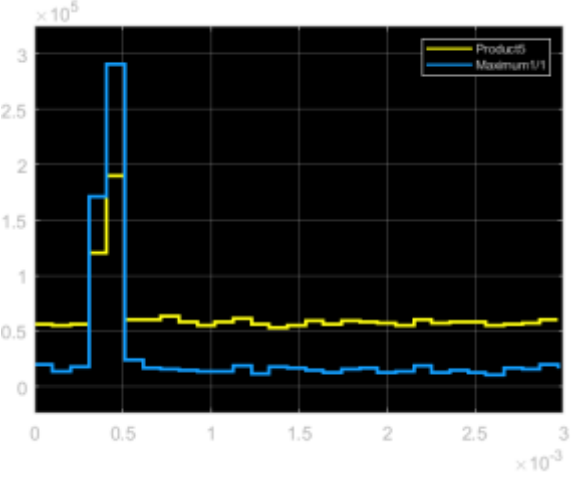

Fig. 6. Compare the maximum correlation result with the threshold.

4. Performance Evaluation

Two main criteria of evaluating the performance of an acquisition algorithm are the detection probability of true code phase offset (τ) and mean acquisition time (T_D). Here in this paper, these items for the proposed algorithm are analyzed with an eye on comparing the results with similar methods in the literature. Detection performance of the long code acquisition method will be investigated. The probability of detection of phase difference (offset) of the code phase is influenced by various parameters, here SNR is considered as the primary parameter and the effect of various factors such as FFT length and Doppler frequency is expressed with different diagrams of detection probability in terms of SNR.

4.1. Detection Performance

Finding the true code phase offset involves correlation of the received signal with a code phase offset of τ and locally generated spreading code with offset of δ. The probability of detection can be obtained either for the entire observation block or for a cell of the observation window.

Detection probability of a single cell is estimated through Neyman-Pearson method, for a given false alarm probability, P_{fa}, the threshold can be derived from

$$P_{fa} = \int_{V_t}^{+\infty} f_\Psi(x|\theta, H_0)dx \qquad (7)$$

With

$$V_t = \sigma_{H_0}\sqrt{-2\ln P_{fa}} \qquad (8)$$

And the detection probability will be [21]:

$$P_d = Q_1\left(\frac{\mu_1}{\sigma_{H_1}}, \frac{V_t}{\sigma_{H_1}}\right) \qquad (9)$$

Where Q_1 is Marcum's Q function and

$$\mu_1^2 = A^2(1-|P|)^2 sinc^2\big(f_D \Delta t(L-N)\big)n^2 \qquad (10)$$

For the ZP method, the detection probability for the entire observation block is obtained from the following equation:

$$V_t = \sqrt{-2\ln P_{fa}(A^2(1-|p|)^2+\sigma^2)(L-N)} \quad (11)$$

$$\mu_1^2 = (L-N)^2A^2 sinc^2\left(\frac{\omega_D}{2}(L-N)\Delta t\right)(1-|p|)^2 \quad (12)$$

$$\sigma_{H_1}^2 = (\sigma^2+A^2p^2)(L-N) \quad (13)$$

as is illustrated in [21], GZP method has the best detection performance and XFAST method has the worst performance in signal detection in terms of FFT length. Additionally, GZP method has the highest Doppler tolerance among the other methods. As a result, The ZP method has been chosen to transmit signal. However, the method suffers from the drawback of a longer acquisition time when compared with other methods since it detects the signal at a very low SNR.

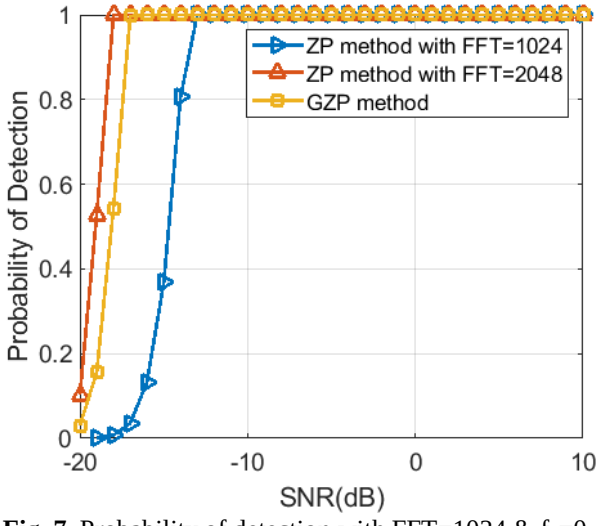

Fig. 7. Probability of detection with FFT=1024 & f_d=0.

The effect of FFT length on probability of detection is shown in Fig.5. In long code acquisition methods, doubling the FFT length improves the detection performance of the ZP method for nearly 3-4dB.

4.2. Mean Acquisition Time

Expected value of the time spent for code acquisition (achieving to desired detection probability) or mean acquisition time for a given false alarm, is a useful measurement for performance comparison of acquisition techniques. The principals of calculating mean acquisition time of an acquisition algorithm are described in [21] for serial search of short codes, which is applicable to long codes as well and is formulated as:

$$E(T_{ACQ}) = \frac{T_D}{P_d^b}\left\{1+\left(1+\gamma P_{fa}^b\right)\left(2-P_d^b\right)\frac{(\wedge-1)}{2}\right\} \quad (14)$$

Where P_d^b and P_{fa}^b are detection and false alarm probability for the block of observation window, respectively. T_D is the dwell time for searching an observation window. $\wedge$ is the number of observation windows in an uncertainty region of θ code phases which is proportional to parallel searching capability of the algorithm that for ZP equals to $\left\lceil\frac{\theta}{N+1}\right\rceil$. Consequently, the mean acquisition time of ZP is obtained from (12) with following parameters:

$$\wedge = \left\lceil\frac{\theta}{N+1}\right\rceil \quad (15)$$

$$P_{fa}^b = 1-\left(1-P_{fa}\right)^N \quad (16)$$

$$P_d^b = 1-\left(1-P_{fa}\right)^{N-1}(1-P_d) \quad (17)$$

Fig. 8 shows the mean acquisition time in T_D. Although GZP has the best performance in terms of detection capabilities, it performs poorly in terms if Mean acquisition time.

As mentioned earlier, the ZP method is a vastly time-consuming technique in the acquisition stage, as is shown in Fig. 6, which verifies the results obtained in [8]. Although the chosen method consumes a lot of acquisition time, what remains of high essence is the signal detection at low SNRs, which increases the acquisition time.

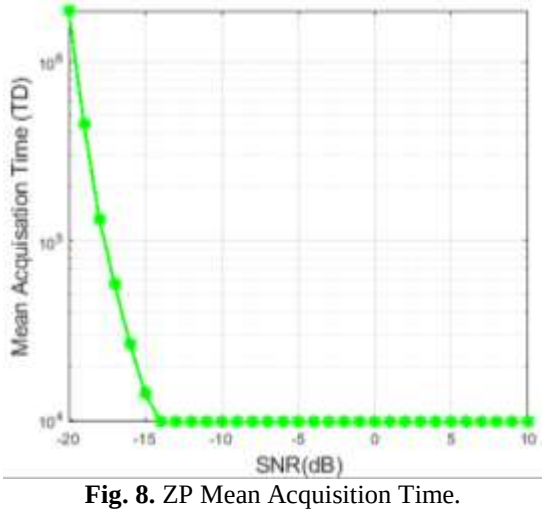

Fig. 8. ZP Mean Acquisition Time.

4.3. Doppler Effect

The residual frequency due to Doppler effect depends on the carrier frequency and the relative speed between the transmitter and the receiver. The residual frequency (usually Doppler) appears in the first argument of the Marcum Q-function as:

$$sinc^2\left(\frac{\omega_D}{2}n\Delta t\right) \qquad (18)$$

According to which, the first zero occurs in $\frac{1}{T_{CI}}$ [21]. therefore, in the ZP method, assuming a chip rate of 10MHz and an FFT length of 1024 samples, the first zero-crossing occurs at approximately 19KHz. Therefore, the Doppler frequency has very little effect on the detection performance of the ZP method.

In the ZP method with the mentioned conditions, Doppler tolerance is equal to [7], [8]:

$$f_d = \frac{f_s}{L-N} = \frac{10^7}{1024-512} = 19KHz \qquad (19)$$

In this work, the receiver is considered to be a UAV flying at the speed of 350 km/h, followed by a subsequent Doppler shift which can be calculated as [19]:

$$f_{doppler} = \frac{V_{UAV}}{\lambda} = 3.5KHz \qquad (20)$$

Therefore, comparison of (17) and (18) shows that doppler effect can be ignored.

As shown in Fig.7, the Doppler effect has a negligible effect on the detection of the ZP method. As the Doppler frequency rises to 20 kHz, the detection probability drops by 2 to 3dB

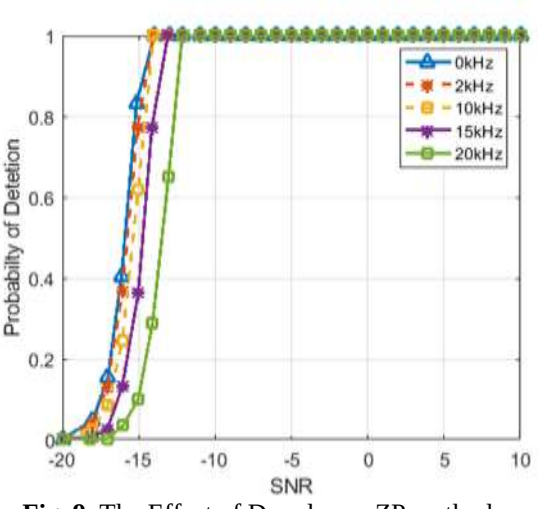

Fig. 9. The Effect of Doppler on ZP method.

5. CONCLUSION

In this paper, Reliable and Robust UAV Data transmission through Geo Satellite using Long Code DSSS with ZP algorithm was simulated and analyzed. The method selected for sending information in this link is the direct sequence spread spectrum technique which meets the transmission requirements in terms of transmission range, fading, and also communication below the noise level, which is of prime importance from a security point of view. The use of this method has caused the desired link to have LPI and LPD characteristics, according to the simulations performed on two performance measurement criteria (Acquisition Time (T_D) and Probability of detection (P_D) in terms of SNR) of Zero padding Algorithm, numerical results were obtained, as shown in fig.7 with increasing the FFT length from 1024 to 2048, P_d value has improved by 4-5dB. Fig.8 shows the acquisition time for FFT length 1024, which is constant acquisition time from SNR= -14dB, which can be derived from equation 14, which shows the accuracy of the simulation method used. Fig. 9 shows the effect of Doppler shift (f_d) on (P_d) of the Zero Padding algorithm in such a way that increasing the f_d to 10 kHz did not change the P_d=0.9 in SNR= -14dB, but increasing the f_d to 15KHz and 20KHz, P_d=0.9 can be achieved in SNR=-13dB, which implies that by increasing f_d up to 20KHz, P_d can be obtained with an increase of 1 dB of SNR, which conforms completely to relations 18 and 19. Also, due to geographical issues, it can send and receive data to places beyond the reach of terrestrial links and can only be accessed through satellite.

REFERENCE

[1] Grekhov, A., Kondratiuk, V. and Ilnytska, S., 2021**. "Data Traffic Modelling in RPAS/UAV Networks with Different Architectures"**. Modelling, 2(2), pp.210-223.

[2] Pai, V.U. and Sainath, B., 2021. **"UAV selection and link switching policy for hybrid tethered UAV-Assisted communication"**. IEEE Communications Letters, 25(7), pp.2410-2414.

[3] Zolanvari, M., Jain, R. and Salman, T., 2020. **"Potential data link candidates for civilian unmanned aircraft systems":** A survey. IEEE Communications Surveys & Tutorials, 22(1), pp.292-319.

[4] Yan, K., Ma, L. and Zhang, Y., 2020, **"December. Research on the Application of 5G Technology in UAV Data Link"**. In 2020 IEEE 9th Joint International Information Technology and Artificial Intelligence Conference (ITAIC) (Vol. 9, pp. 1115-1118). IEEE.

[5] He, Y., Zhai, D., Zhang, R., Du, X. and Guizani, M., 2019. **"An Anti-Interference Scheme for UAV Data Links in Air–Ground Integrated Vehicular Networks".** Sensors, 19(21), p.4742.and Control Simulation (MECS 2017) (pp. 268-276). Atlantis Press.

[6] Tubbal, F.E.M., Alkaseh, A. and Elarabi, A., 2015, November. **"Telemetry, tracking and command subsystem for LibyaSat-1"**. In 2015 9th International Conference on Telecommunication Systems Services and Applications (TSSA) (pp. 1-6). IEEE.

[7] Amiri, H. and Khaleghi Bizaki, H., 2017. **"Compensation of Doppler Effect in Direct Acquisition of Global Positioning System using Segmented Zero Padding".** Journal of Communication Engineering, 6(2), pp.118-130.

[8] Ping, J., Wu, X., Yan, J. and Zhu, W., 2014, September. **"Modified zero-padding method for fast long PN-code acquisition".** In 2014 IEEE 80th Vehicular Technology Conference (VTC2014-Fall) (pp. 1-5). IEEE.

[9] Geiger, B.C. and Vogel, C., 2013., **"Influence of Doppler bin width on GPS acquisition probabilities".** IEEE transactions on aerospace and electronic systems, 49(4), pp.2570-2584.
[10] Simone, L., Fittipaldi, G. and Sanchez, I.A., 2011, November. **"Fast acquisition techniques for very long PN codes for on-board secure TTC transponders"**. In 2011-MILCOM 2011 Military Communications Conference (pp. 1748-1753). IEEE.
[11] Guoliang, S., 2009, March. **"A fast acquisition method of DSSS signal based on double FFT layers".** In 2009 WRI World Congress on Computer Science and Information Engineering (Vol. 1, pp. 452-456). IEEE.
[12] Li, H., Lu, M., Cui, X. and Feng, Z., 2009. **"Generalized zero-padding scheme for direct GPS P-code acquisition"**. IEEE transactions on wireless communications, 8(6), pp.2866-2871.
[13] Iinatti, J.H., 2000. **"On the threshold setting principles in code acquisition of DS-SS signals"**. IEEE Journal on selected Areas in Communications, 18(1), pp.62-72.
[14] ETSI, E., 2005. Digital video broadcasting (dvb); second generation framing structure, channel coding and modulation systems for broadcasting, interactive services, news gathering and other broadband satellite applications. Part II: S2-Extensions (DVB-S2X), pp.22-27.
[15] Ziemer, R.E., 2007. **"Fundamentals of spread spectrum modulation".** Synthesis Lectures on communications, 2(1), pp.1-79.
[16] Li, H., Lu, M., Cui, X. and Feng, Z., 2009. **"Generalized zero-padding scheme for direct GPS P-code acquisition"**. IEEE transactions on wireless communications, 8(6), pp.2866-2871.
[17] Iinatti, J.H., 2000. **"On the threshold setting principles in code acquisition of DS-SS signals"**. IEEE Journal on selected Areas in Communications, 18(1), pp.62-72.
[18] Borna, M. and Madani, M.H., 2016. **"Improving Long PN-Code Acquisition in the Presence of Doppler Frequency Shifts"**. AUT Journal of Electrical Engineering, 48(1), pp.19-27.
[19] Maral, G., Bousquet, M. and Sun, Z., 2020. **"Satellite communications systems: systems",** techniques and technology. John Wiley & Sons.
[20] Pratt, T. and Allnutt, J.E., 2019. Satellite communications. John Wiley & Sons.
[21] Kaplan, E.D. and Hegarty, C. eds., 2017. Understanding GPS/GNSS: principles and applications. Artech house.
[22] Pan, J., Zheng, L., Li, H. and Wang, T., 2016, June. **"Design of Spread Spectrum TT&C Link for UAV-Swarm Based on Multi-path**". In 2017 2nd International Conference on Machinery, Electronics